# Remarkable Shifts of C$_{sp2}$-H and O-H Stretching Frequencies and Stability of Complexes of Formic Acid with Formaldehydes and Thioformaldehydes

Nguyen Tien Trung [iD],*[a] Pham Ngoc Khanh,[a] Alfredo J. Palace Carvalho,[b] and Minh Tho Nguyen[c]

Thirty-six stable complexes of formic acid with formaldehydes and thioformaldehydes were determined on the potential energy surface, in which the XCHO···HCOOH complexes are found to be more stable than the XCHS···HCOOH counterparts, with **X** = H, F, Cl, Br, CH$_3$, NH$_2$. All complexes are stabilized by hydrogen bonds, and their contribution to the total stabilization energy of the complexes increases in going from C-H···S to C-H···O to O-H···S and finally to O-H···O. Remarkably, a significant blueshift of C$_{sp2}$-H bond by 81–96 cm$^{-1}$ in the C$_{sp2}$-H···O hydrogen bond has hardly ever been reported, and a considerable redshift of O-H stretching frequency by 206–544 cm$^{-1}$ in the O-H···O/S hydrogen bonds is also predicted. The obtained results in our present work and previous literatures support that a distance contraction and a stretching frequency blueshift of C-H bond involving hydrogen bond depend mainly on its polarity and gas phase basicity of proton acceptor, besides the rearrangement of electron density due to complex formation. Markedly, we suggest the ratio of deprotonation enthalpy to proton affinity ($R_c$) as an indicator to prospect for classification of hydrogen bonds. The symmetry adapted perturbation theory results show a larger role of attractive electrostatic term in **XO-n** as compared to that in **XS-n** and the electrostatic interaction is overwhelming dispersion or induction counterparts in stabilizing **XO-n** and **XS-n**, with **n** = 1, 2, 3. © 2019 Wiley Periodicals, Inc.

## Introduction

Noncovalent interactions are an essential factor in many fields such as crystal packing, molecular recognition, biological processes, and reaction selectivity.[1] Among of the known interactions, the A-H···B hydrogen bond is of major general interest arising from its crucial role in many fields of chemistry, physics, and biology, especially in nature.[2,3] Its importance has even more comprehensively been recognized when the presence of C-H···O/N hydrogen bonds was discovered in proteins, DNA double helix, RNA, and so forth.[2–4] More meaningfully, the existence of C-H···π, C-H···halogen bonds has been found in molecular clusters, enzymatic mechanism, crystal packing, and so forth.[5–8] A recent study confirmed both experimentally and theoretically for the first time that the C-H···S bond exists between an enzyme methionine aminopeptidase and its N-terminal-methionine polypeptide substrate.[9] This result indicates the unique functional role of the C-H···S bond in the substrate specificity and enzyme catalysis of type 1 methionine aminopeptidase.

Normally, formation of a hydrogen bond weakens the donor A-H bond, causing an elongation of the A-H distance and a concomitant lowering of the A-H stretching frequency as compared to the original A-H monomer. Its origin is well understood that is due to an electrostatic interaction between H and B atoms. This type of hydrogen bond is conventionally referred as a red-shifting hydrogen bond (RSHB). However, a number of experimental and theoretical studies have demonstrated that an A-H···B formation can lead to an unexpected distance contraction and stretching frequency blueshift of an A-H covalent bond.[10–12] This phenomenon results in another kind of hydrogen bond, called blue-shifting hydrogen bond (BSHB). BSHB has often been revealed in systems where a hydrogen atom bonded to a carbon atom, and forms a hydrogen bond with either an electronegative atom or a region having an excess of electron density. Several investigations concerning this type of hydrogen bond have indeed been performed both experimentally and theoretically.[13–20] Focusing on hydrogen-bonded systems containing the C-H···O and/or C-H···N bonds, these previous studies aimed at classification of hydrogen bonds and understanding of their origin.[21–25] The obtained results helped us to rationalize the physicochemical nature of C-H···O/N bonds and evaluate their contribution to the overall stability of nucleobase pairs and protein–DNA/RNA molecular recognition processes, that are of potential importance for unraveling the mysteries of cellular functions in various diseases, as well as for development of new drugs.

[a] N. Tien Trung, P. Ngoc Khanh
    Laboratory of Computational Chemistry and Modelling, and Department of Chemistry, Quy Nhon University, Quy Nhon, Vietnam
    E-mail: nguyentientrung@qnu.edu.vn

[b] A. J. P. Carvalho
    Department of Chemistry, School of Sciences and Technology, and Évora Chemistry Center, IIFA, University of Évora, Évora, Portugal

[c] M. Tho Nguyen
    Department of Chemistry, KU Leuven, Celestijnenlaan 200F, B-3001, Leuven, Belgium

**Wiley Online Library**

*J. Comput. Chem.* **2019**, *40*, 1387–1400    **1387**

Heretofore, several hypotheses have been proposed to rationalize the BSHB phenomenon.[10,11,26,27] Let us mention two recent viewpoints. A theoretical study suggested that the trend of A-H stretching frequency shifts is caused by a competition between the electrostatic and hyperconjugative interactions.[28] Another study reported that when a proton acceptor interacts with a proton donor, the covalent characteristic of A-H bond causes a blueshift, while its ionic property results in a redshift.[29] Competition of two factors tends thus to govern the change in stretching vibrational frequency of the A-H bond. In general, each hypothesis has some specific advantages and limitations, and they all rationalize the phenomenon on the basis of dimer properties when a hydrogen-bonded complex is already formed.

We have pursued another approach to study the origin of the BSHB and, thereby, a classification of hydrogen bonds, which is rather based on inherent properties of isolated monomers. Implementing this approach, the stability and origin of hydrogen bond involving C-H covalent bond have been explored.[24,30,31] Our theoretical results obtained for the hydrogen-bonded systems containing C-H⋯O/N suggested that the origin of a BSHB in a A-H⋯B complex can be probed on the basis of the deprotonation enthalpy (DPE) of the A-H bond in the isolated proton donor and the proton affinity (PA) of the B atom in the isolated proton acceptor.[32–34] Notably, the BSHB is usually observed in complexes between C-H group acting as a proton donor both experimentally and theoretically.[12,35] Accordingly, it is believed that the origin BSHB and classification of the hydrogen bond can be elucidated based on the understanding of the basis of stability and origin of hydrogen bond involving $C_{sp2}$-H bond.

In an attempt to pursue further this approach, we set out to perform a systematic investigation on the molecular complexes formed by formic acid (HCOOH) with substituted formaldehydes and thioformaldehydes (XCHZ, with X = H, F, Cl, Br, $CH_3$, $NH_2$, and Z = O, S). To the best of our knowledge, a systematic investigation into these complexes at the molecular level has not been reported yet. In addition, a study on BSHB involved in $C_{sp2}$-H species, especially the type of $C_{sp2}$-H⋯S, has rarely been reported, even though some studies on the C-H⋯S complexes with different hybridized carbon atoms were recorded.[36–40] More importantly, the main purpose of the present work is an evaluation of substituent effects of various X groups in the XCHO and XCHS compounds on the characteristics of C-H⋯O/S and O-H⋯O/S hydrogen-bonded interactions, and their role in stabilization of XCHZ⋯HCOOH complexes on the basis of the polarizability of the C-H covalent bond and gas phase basicity of the O and S atoms. The obtained results also emphasize the similarities and differences of substituted formaldehydes and thioformaldehydes in their complexation with formic acid. Overall, calculated changes of C-H bond lengths, stretching vibrational frequencies and their correlations with electronic properties of relevant monomers and complexes allow us to probe further the origin of the high stability of the considered complexes and their remarkable $C_{sp2}$-H⋯O/S BSHBs.

## Computational Methods

Geometry optimizations for all investigated structures including the monomers and complexes are carried out using the second-order Møller–Plesset perturbation theory (MP2) with the correlation consistent aug-cc-pVDZ basis set. This level of theory is selected in the present work on the basis of a comparison of calculated results including geometric parameters, proton affinities and DPEs given in Table 1 and Table S1 (Supporting Information) for the XCHZ and HCOOH monomers with available experimental results listed in the NIST webpage.[41] Geometries are fully optimized without symmetry constraint. Harmonic vibrational frequencies are subsequently performed at the same level to identify the equilibrium structures and to estimate their zero-point energies (ZPEs). Harmonic stretching frequencies of C-H bonds in HCHO and HCHS are calculated according to isotopomers for both monomers and their complexes in order to avoid vibrational coupling of $CH_2$ group stretching. Single point electronic energies of monomers and complexes are evaluated using the coupled-cluster theory CCSD(T) with the aug-cc-pVDZ basis set making use of MP2/aug-cc-pVDZ optimized geometries. The interaction energy of each complex investigated is determined as the difference in electronic energies of the complex and the corresponding monomers, which are corrected for ZPEs and basis set superposition errors (BSSEs). The latter is computed using the Boys and Bernadi scheme[42] with the CCSD(T)/aug-cc-pVDZ method and MP2/aug-cc-pVDZ geometries. All calculations mentioned above are carried out employing the Gaussian 09 suite of program.[43]

Symmetry adapted perturbation theory (SAPT2+) calculations are computed using the PSI4 program[44] with the aug-cc-pVDZ basis set to unravel the contribution of different energy components to the stability of complexes. Individual components of interaction energy include the electrostatic ($E_{elst}$), induction ($E_{ind}$), dispersion ($E_{disp}$), exchange ($E_{exch}$) terms, and $\delta E_{int,r}^{HF}$ terms, where $\delta E_{int,r}^{HF}$ contains the third and higher order induction and exchange-induction contributions. Interaction energies based on the SAPT2+ approach (denoted by $\Delta E_{SAPT2+}$) are calculated according to eq. (1):

$$\Delta E_{SAPT2+} = E_{elst} + E_{exch} + E_{ind} + E_{disp} + \delta E_{int,r}^{HF} \quad (1)$$

The atoms-in-molecules approach (AIM),[45] to search critical points of the electron density and their Laplacians, is performed at the MP2/aug-cc-pVDZ level. The local electron energy density ($H(r)$) at a bond critical point (BCP) is computed by eq. (2):

$$H(r) = G(r) + V(r) \quad (2)$$

in which $V(r)$ and $G(r)$ are the corresponding electron potential and kinetic energy density, respectively.

Individual energy of each hydrogen bond ($E_{HB}$) is estimated by means of eq. (3):

$$E_{HB} = 0.5V(r) \quad (3)$$

as suggested by Espinosa–Molins–Lecomte.[46,47] The natural bond orbital (NBO) analysis using the NBO 5.G[48] software integrated in Gaussian 09 program is also performed to identify the presence, and to correlate the thermodynamical stability of hydrogen-bonded interactions and electron density transfers upon complex formation.

**Table 1.** Some selected parameters of monomers at MP2/aug-cc-pVDZ.

| Monomer | HCHO | FCHO | ClCHO | BrCHO | CH₃CHO | NH₂CHO |
|---|---|---|---|---|---|---|
| $r$(C-H)/Å | 1.1116 | 1.1010 | 1.1041 | 1.1048 | 1.1167 | 1.1119 |
| $r$(C-H)[a]/Å | 1.111 | 1.095 | – | – | 1.1140 | – |
| $r$(C=O)/Å | 1.2237 | 1.1936 | 1.1987 | 1.1983 | 1.2260 | 1.2281 |
| $r$(C=O)[a]/Å | 1.205 | 1.181 | – | – | 1.216 | – |
| $q$(C)/e | 0.28 | 0.78 | 0.39 | 0.33 | 0.43 | 0.55 |
| $q$(H)/e | 0.11 | 0.13 | 0.17 | 0.17 | 0.12 | 0.12 |
| $q$(O)/e | −0.51 | −0.52 | −0.47 | −0.46 | −0.53 | −0.61 |
| σ*(C-H)/e | 0.0678 | 0.0727 | 0.0732 | 0.0715 | 0.0784 | 0.0795 |
| $E_{intra}$(n(O) → σ*(C-H))/kJ mol⁻¹ | 108.4 | 110.3 | 114.1 | 112.4 | 123.7 | 126.5 |
| $E_{intra}$(n(X) → σ*(C-H))/kJ mol⁻¹ | – | 23.5 | 16.9 | 11.9 | – | – |
| PA(O)/kJ mol⁻¹ | 712.9 | 662.5 | 694.4 | 704.9 | 772.2 | 834.3 |
| PA(O)[a]/kJ mol⁻¹ | 711.5 ± 2.1 | – | – | – | 768.5 | 822.2 |
| DPE(C-H)[b]/kJ mol⁻¹ | 1677.1 | 1571.1 | 1530.3 | 1499.2 | 1656.0 | 1644.4 |
| DPE(C-H)[a]/kJ mol⁻¹ | 1650.7 ± 0.96 | 1475.0 ± 19 | | | 1645.1 ± 4.0 | 1505.0 ± 8.8 |
| **Monomer** | **HCHS** | **FCHS** | **ClCHS** | **BrCHS** | **CH₃CHS** | **NH₂CHS** |
| $r$(C-H)/Å | 1.0987 | 1.0980 | 1.0972 | 1.0972 | 1.1026 | 1.1006 |
| $r$(C-H)[a]/Å | 1.087 | – | – | – | 1.0890 | – |
| $r$(C=S)/Å | 1.6308 | 1.6100 | 1.6192 | 1.6183 | 1.6354 | 1.6492 |
| $r$(C=S)[a]/Å | 1.611 | – | – | – | 1.610 | |
| $q$(C)/e | −0.48 | 0.10 | −0.38 | −0.47 | −0.29 | −0.11 |
| $q$(H)/e | 0.19 | 0.18 | 0.22 | 0.22 | 0.20 | 0.20 |
| $q$(S)/e | 0.09 | 0.07 | 0.15 | 0.17 | 0.07 | −0.11 |
| σ*(C-H)/e | 0.0473 | 0.0627 | 0.0623 | 0.0605 | 0.0562 | 0.0588 |
| $E_{intra}$(n(S) → σ*(C-H))/kJ mol⁻¹ | 66.1 | 69.0 | 71.4 | 71.6 | 76.9 | 73.6 |
| $E_{intra}$(n(X) → σ*(C-H))/kJ mol⁻¹ | – | 31.6 | 25.9 | 19.3 | – | – |
| PA(S)/kJ mol⁻¹ | 766.4 | 723.5 | 755.2 | 764.6 | 808.2 | 856.8 |
| PA(S)[a]/kJ mol⁻¹ | 759.7 | – | – | – | – | – |
| DPE(C-H)[b]/kJ mol⁻¹ | 1630.6 | 1567.8 | 1528.1 | 1497.5 | 1626.4 | 1604.1 |
| DPE(C-H)[a]/kJ mol⁻¹ | – | – | – | – | 1461.0 ± 17 | – |

Values of PA and DPE at CCSD(T)/aug-cc-pVTZ//MP2/aug-cc-pVDZ; $n$ denoted for lone pair of electron; $q$ denoted for NBO charge; $r$ denoted for bond length; $E_{intra}$ denoted for intramolecular hyperconjugative energy.
[a] For experimental values taken from NIST webpage.[39]
[b] The values of DPE of C-H bond taken from optimized geometry of monomer with only removing proton of C-H bond, without XCO anion reoptimization (due to their XCO or XCS anions nonstability).

## Results and Discussion

### Geometric structures of monomers and complexes, and AIM analysis

As shown in Table 1, substitution of one H atom in both HCHZ (Z = O, S) by halogen atoms (F, Cl, Br) tends to slightly shorten the C-H bond distance by 0.0007–0.0106 Å, in contrast to the case of H replacement by CH₃ or NH₂ group in which it induces a marginal lengthening of C-H bond by 0.0003–0.0051 Å, and in comparison to C-H bond length in relevant HCHZ monomers. The changing trends of C-H bond lengths in HCHZ are in agreement with the previous report on rehybridization trend of C atom when H atom is substituted by more electronegative or electropositive atoms.[49] This replacement also causes a similar trend of >C=O and >C=S bond lengths in HCHZ when one H atom is substituted by an X. Indeed, a decrease of 0.0116–0.0301 Å (X = halogens), and an increase of 0.0023–0.0184 Å (X = CH₃, NH₂) for the >C=Z bond lengths are found. Accordingly, the replacement of electron donating CH₃ and NH₂ group leads to an increase of C-H and >C=Z distances, whereas a decrease is induced when X is substituted by the electron withdrawing F, Cl, Br atoms.

NBO charges of C and H atoms in XCHO at MP2/aug-cc-pVDZ (cf. Table 1) are in turn in the range of 0.29–0.78 electron and 0.11–0.17 electron, and they range from −0.48 to 0.10 electron

and 0.18 to 0.22 electron in XCHS. This confirms that the polarity of C-H bond is stronger for XCHS than for XCHO with the same substituent X. The O atoms of XCHO are negatively charged in going from −0.46 to −0.61 electron, while the positive charges of S atoms are in the range of 0.07–0.17 electron for all XCHS monomers, except for a small negative charge of 0.11 electron for NH₂CHS. Consequently, O atoms of XCHO have a stronger propensity for attractive electrostatic interaction with positively charged donors.

We now consider the complexes of XCHZ monomers and HCOOH for an evaluation of substituent effects on various monomeric and dimeric properties. Interaction of HCOOH with XCHZ induces 36 stable complexes having three distinct geometric shapes, denoted hereafter by **XZ-n**, with **X** = H, F, Cl, Br, CH₃, NH₂; **Z** = O, S; and **n** = 1–3, and their topological features are displayed in Figure 1. Intermolecular contact distances of complexes and selected results of an AIM analysis (MP2/aug-cc-pVDZ) are collected in Table 2.

Each complex is stabilized by two intermolecular contacts including C5-H6···Z3 and C1-H2···O7 in **XZ-1**, C5-H6···Z3 and C1-H2···O8 in **XZ-2**, and C1-H2···O7 and O8-H9···Z3 in **XZ-3**. All H6/H9···O3, H6/H9···S3, and H2···O7/O8 intermolecular distances are in the range of 1.68–2.57 Å, 2.23–3.02 Å, and 2.17–2.60 Å, respectively, that in general are shorter or close to the sums of van der Waals radii of relevant atoms (being 2.72
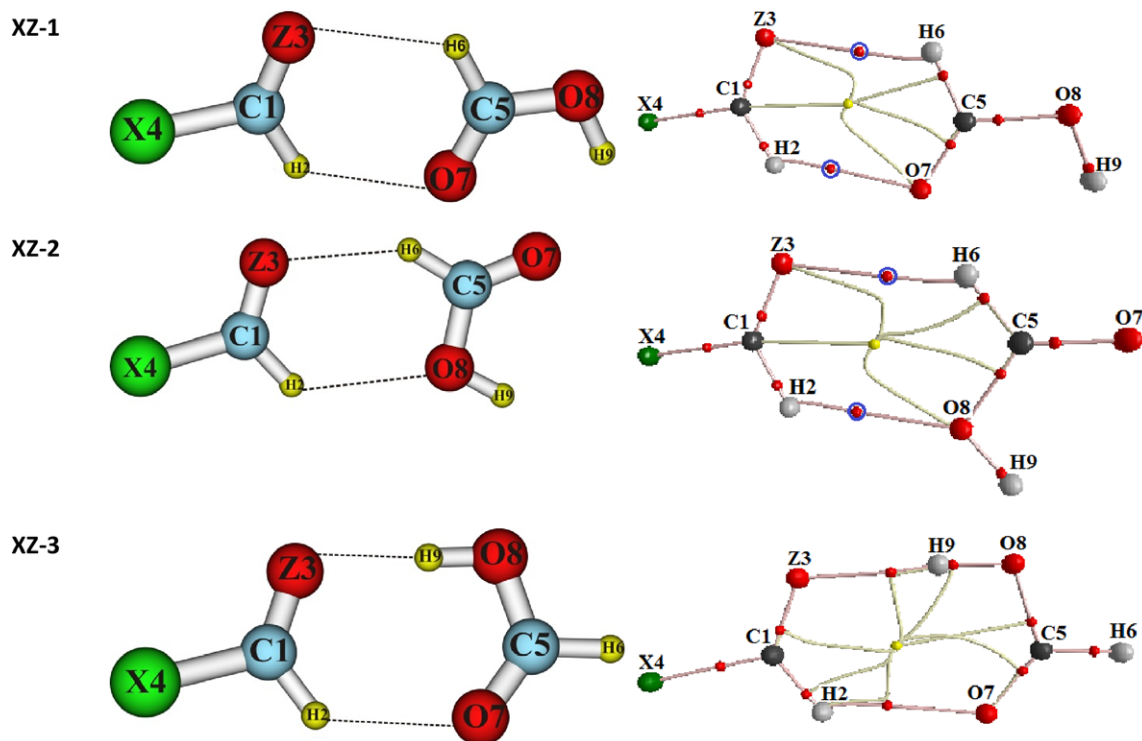
**Wiley Online Library**

*J. Comput. Chem.* **2019**, *40*, 1387–1400 **1389**

**Figure 1.** Optimized geometries and topological features of complexes upon interactions of HCOOH with XCHZ (**X** = H, F, Cl, Br, CH₃, NH₂; **Z** = O, S) at MP2/aug-cc-pVDZ. [Color figure can be viewed at wileyonlinelibrary.com]

and 3.0 Å for H⋯O and H⋯S corresponding contacts, respectively). This roughly suggests the presence of these intermolecular interactions in the considered complexes. The existence of H6⋯S3 contacts in complexes **FS-1** (3.02 Å), **ClS-1** (3.01 Å), and **BrS-1** (3.01 Å) is due to an additional cooperative contribution of the rest of interaction. As seen in Table 2, H⋯O distances of C-H⋯O intermolecular contacts are comparable to those in the dimers of HCHO⋯HCHO (2.44 Å), CH₃CHO⋯CH₃CHO (2.40 Å), and CF₃CHO⋯CH₃CHO (2.45 Å) previously computed at the MP2/aug-cc-pVTZ level,[50] and HCHO⋯HCHO (2.47 Å) at the ae-CCSD(T)/cc-pwCV5Z level.[51] Additionally, present values of H⋯O distances of O-H⋯O contacts are also close to those reported in the literature[52] including 1.73 Å (1.68 Å) and 1.71 Å (1.67 Å) for (HCOOH)₂ and (CH₃COOH)₂ at the MP2/6-311++G (d,p) (values in brackets at MP2/aug-cc-pVDZ). Furthermore, evidence for existence of these interactions is confirmed by the presence of BCPs of the intermolecular contacts as shown in Figure 1. All values of electron density ($\rho(r)$) and Laplacian ($\nabla^2(\rho(r))$) at these BCPs are in the range of 0.0067–0.0281 and 0.018–0.151 au, except for the BCPs of H9⋯O3 contacts in **HO-3**, **CH₃O-3**, and **NH₂O-3** having larger electron densities of 0.0367, 0.0401, and 0.0455 au, respectively. All of them fall within the limitation criteria for the formation of weak interactions suggested by Popelier and Koch.[53] Hence, the C5-H6⋯Z3 and C1-H2⋯O7 in **XZ-1**, C5-H6⋯Z3 and C1-H2⋯O8 in **XZ-2**, and C1-H2⋯O7 and O8-H9⋯Z3 in **XZ-3** are characterized as hydrogen bonds. This result is also affirmed by the positive values of local electron energy densities ($H(r)$) at these BCPs in the complexes investigated. The magnitude in strength of hydrogen bonds increases in the ordering of C-H⋯S to C-H⋯O to

O-H⋯S and then to O-H⋯O. This observation is also supported by a directly proportional linear correlation of individual hydrogen bond energies ($E_{HB}$) with respect to H⋯Z distances (R(H⋯Z)) in the complexes examined, as displayed in Figure 2. Strikingly, very large values of $\rho(r)$ and negative values of $H(r)$ at BCPs of O8-H9⋯O3 contacts are found in **HO-3**, **CH₃O-3**, and **NH₂O-3**, implying that these strong hydrogen bonds are partly covalent in nature.[54,55] Such an observation on partly covalent property of hydrogen bond is consistent with previous results on (HCOOH)₂ and (CH₃COOH)₂ dimers.[51]

In an attempt to understand the correlationship between hydrogen bond energies ($E_{HB}$) with electron densities ($\rho(r)$) at BCPs of H⋯Z contacts and hydrogen-bonded distances (R (H⋯Z)), these correlations are presented in Figure 3. A second-order inverse correlation of $E_{HB}$ versus $\rho(r)$ is hence obtained. It shows that the more negative $E_{HB}$ becomes, the more stable complex is, when $\rho(r)$ increases, and vice versa. In other words, the larger the electron density at BCPs, the stronger the C(O)-H⋯Z hydrogen-bonded interaction. On the contrary, a second-order direct correlation is found between $E_{HB}$ and R(H⋯Z) (Fig. 3). It presents that $E_{HB}$ increases when R(H⋯Z) increases, and the stability of C(O)-H⋯Z hydrogen bonds decreases when intermolecular distances of H⋯Z contacts increases, and vice versa.

In summary, all the 36 complexes located are stabilized by two hydrogen bonds which are C1-H2⋯O7 and C5-H6⋯Z3 in **XZ-1**, C1-H2⋯O8 and C5-H6⋯Z3 in **XZ-2**, and C1-H2⋯O7 and O8-H9⋯Z3 in **XZ-3**, with **Z** = O and S. The largest contribution to stability of the complexes formed by interaction of

**Table 2.** Intermolecular distances R(H⋯Z), selected parameters at the BCPs of H⋯Z (**Z** = O, S) contacts at MP2/aug-cc-pVDZ and individual hydrogen-bond energies ($E_{HB}$).

| Complex | Contacts | R(H⋯Z) (Å) | $\rho(r)$ (au) | $\nabla^2\rho(r)$ (au) | $H(r)$[a] (au) | $E_{HB}$[b] (kJ mol$^{-1}$) |
|---|---|---|---|---|---|---|
| **HO-1** | C1-H2⋯O7 | 2.50 | 0.0097 | 0.030 | 0.0003 | −9.3 |
| | C5-H6⋯O3 | 2.42 | 0.0114 | 0.035 | 0.0001 | −11.1 |
| **HO-2** | C1-H2⋯O8 | 2.59 | 0.0073 | 0.027 | 0.0007 | −6.8 |
| | C5-H6⋯O3 | 2.38 | 0.0122 | 0.035 | 0 | −11.6 |
| **HO-3** | C1-H2⋯O7 | 2.37 | 0.0128 | 0.039 | 0.0001 | −12.5 |
| | O8-H9⋯O3 | 1.77 | 0.0367 | 0.127 | −0.0011 | −38.6 |
| **HS-1** | C1-H2⋯O7 | 2.37 | 0.0119 | 0.035 | 0 | −11.4 |
| | C5-H6⋯S3 | 2.90 | 0.0083 | 0.022 | 0.00048 | −5.8 |
| **HS-2** | C1-H2⋯O8 | 2.45 | 0.0091 | 0.031 | 0.00048 | −8.8 |
| | C5-H6⋯S3 | 2.84 | 0.0092 | 0.023 | 0.00041 | −6.4 |
| **HS-3** | C1-H2⋯O7 | 2.27 | 0.0145 | 0.043 | 0 | −14.1 |
| | O8-H9⋯S3 | 2.30 | 0.0235 | 0.051 | 0.0004 | −15.7 |
| **FO-1** | C1-H2⋯O7 | 2.37 | 0.0124 | 0.039 | 0.0002 | −12.2 |
| | C5-H6⋯O3 | 2.55 | 0.0086 | 0.030 | 0.0006 | −8.2 |
| **FO-2** | C1-H2⋯O8 | 2.46 | 0.0095 | 0.034 | 0.0007 | −9.2 |
| | C5-H6⋯O3 | 2.50 | 0.0093 | 0.030 | 0.0004 | −8.8 |
| **FO-3** | C1-H2⋯O7 | 2.32 | 0.0137 | 0.043 | 0.0003 | −13.5 |
| | O8-H9⋯O3 | 1.87 | 0.0278 | 0.100 | 0.0022 | −27.0 |
| **FS-1** | C1-H2⋯O7 | 2.27 | 0.0143 | 0.042 | 0 | −13.9 |
| | C5-H6⋯S3 | 3.02 | 0.0067 | 0.018 | 0.0006 | −4.5 |
| **FS-2** | C1-H2⋯O8 | 2.35 | 0.0111 | 0.036 | 0.0004 | −10.8 |
| | C5-H6⋯S3 | 2.96 | 0.0075 | 0.019 | 0.0005 | −5.0 |
| **FS-3** | C1-H2⋯O7 | 2.22 | 0.0158 | 0.047 | 0 | −15.4 |
| | O8-H9⋯S3 | 2.37 | 0.0195 | 0.044 | 0.0007 | −12.6 |
| **ClO-1** | C1-H2⋯O7 | 2.35 | 0.0131 | 0.040 | 0 | −12.8 |
| | C5-H6⋯O3 | 2.55 | 0.0085 | 0.029 | 0.0006 | −8.0 |
| **ClO-2** | C1-H2⋯O8 | 2.44 | 0.0099 | 0.035 | 0.0007 | −9.6 |
| | C5-H6⋯O3 | 2.50 | 0.0093 | 0.029 | 0.0004 | −8.7 |
| **ClO-3** | C1-H2⋯O7 | 2.30 | 0.0144 | 0.044 | 0 | −14.1 |
| | O8-H9⋯O3 | 1.87 | 0.0281 | 0.099 | 0.0021 | −27.2 |
| **ClS-1** | C1-H2⋯O7 | 2.24 | 0.0154 | 0.044 | 0 | −14.9 |
| | C5-H6⋯S3 | 3.01 | 0.0069 | 0.019 | 0.0006 | −4.7 |
| **ClS-2** | C1-H2⋯O8 | 2.32 | 0.0119 | 0.038 | 0.0004 | −11.6 |
| | C5-H6⋯S3 | 2.94 | 0.0077 | 0.020 | 0.0005 | −5.2 |
| **ClS-3** | C1-H2⋯O7 | 2.18 | 0.0171 | 0.050 | 0 | −16.7 |
| | O8-H9⋯S3 | 2.35 | 0.0206 | 0.046 | 0.0007 | −13.4 |
| **BrO-1** | C1-H2⋯O7 | 2.32 | 0.0138 | 0.041 | 0 | −13.5 |
| | C5-H6⋯O3 | 2.57 | 0.0082 | 0.029 | 0.0006 | −7.7 |
| **BrO-2** | C1-H2⋯O8 | 2.43 | 0.0104 | 0.035 | 0.0006 | −10.0 |
| | C5-H6⋯O3 | 2.51 | 0.0090 | 0.029 | 0.0004 | −8.4 |
| **BrO-3** | C1-H2⋯O7 | 2.29 | 0.0148 | 0.045 | 0 | −14.5 |
| | O8-H9⋯O3 | 1.88 | 0.0276 | 0.097 | 0.0021 | −26.6 |
| **BrS-1** | C1-H2⋯O7 | 2.22 | 0.0159 | 0.045 | 0 | −15.5 |
| | C5-H6⋯S3 | 3.01 | 0.0068 | 0.019 | 0.0006 | −4.6 |
| **BrS-2** | C1-H2⋯O8 | 2.30 | 0.0124 | 0.039 | 0.0003 | −12.1 |
| | C5-H6⋯S3 | 2.94 | 0.0077 | 0.020 | 0.0005 | −5.2 |
| **BrS-3** | C1-H2⋯O7 | 2.17 | 0.0175 | 0.051 | 0 | −17.1 |
| | O8-H9⋯S3 | 2.35 | 0.0205 | 0.046 | 0.0006 | −13.4 |
| **CH$_3$O-1** | C1-H2⋯O7 | 2.51 | 0.0095 | 0.029 | 0.0002 | −9.0 |
| | C5-H6⋯O3 | 2.36 | 0.0127 | 0.037 | 0 | −12.4 |
| **CH$_3$O-2** | C1-H2⋯O8 | 2.60 | 0.0071 | 0.026 | 0.0007 | −6.6 |
| | C5-H6⋯O3 | 2.33 | 0.0134 | 0.037 | 0 | −12.9 |
| **CH$_3$O-3** | C1-H2⋯O7 | 2.36 | 0.0130 | 0.039 | 0 | −21.6 |
| | O8-H9⋯O3 | 1.74 | 0.0401 | 0.136 | −0.0003 | −43.8 |
| **CH$_3$S-1** | C1-H2⋯O8 | 2.36 | 0.0122 | 0.035 | 0 | −11.8 |
| | C5-H6⋯S3 | 2.86 | 0.0089 | 0.023 | 0.0005 | −6.3 |
| **CH$_3$S-2** | C1-H2⋯O8 | 2.43 | 0.0094 | 0.031 | 0.0005 | −9.1 |
| | C5-H6⋯S3 | 2.81 | 0.0097 | 0.024 | 0.0004 | −6.9 |
| **CH$_3$S-3** | C1-H2⋯O7 | 2.25 | 0.0151 | 0.044 | 0 | −14.6 |
| | O8-H9⋯S3 | 2.28 | 0.0246 | 0.053 | 0.0002 | −16.7 |
| **NH$_2$O-1** | C1-H2⋯O7 | 2.48 | 0.0101 | 0.031 | 0.0002 | −9.7 |
| | C5-H6⋯O3 | 2.30 | 0.0141 | 0.041 | 0 | −13.9 |
| **NH$_2$O-2** | C1-H2⋯O8 | 2.27 | 0.0075 | 0.027 | 0.0007 | −7.0 |
| | C5-H6⋯O3 | 2.56 | 0.0148 | 0.041 | 0 | −14.3 |
| **NH$_2$O-3** | C1-H2⋯O7 | 2.32 | 0.0140 | 0.042 | 0 | −13.7 |

*(Continues)*

**Wiley Online Library**

*J. Comput. Chem.* **2019**, *40*, 1387–1400     **1391**

**Table 2.** Continued

| Complex | Contacts | R(H⋯Z) (Å) | $\rho(r)$ (au) | $\nabla^2\rho(r)$ (au) | $H(r)$[a] (au) | $E_{HB}$[b] (kJ mol$^{-1}$) |
|---|---|---|---|---|---|---|
| | O8-H9⋯O3 | 1.68 | 0.0455 | 0.151 | −0.0014 | −53.1 |
| **NH$_2$S-1** | C1-H2⋯O8 | 2.31 | 0.0135 | 0.039 | 0 | −13.0 |
| | C5-H6⋯S3 | 2.80 | 0.0098 | 0.025 | 0.0004 | −7.0 |
| **NH$_2$S-2** | C1-H2⋯O8 | 2.39 | 0.0101 | 0.033 | 0.0004 | −9.8 |
| | C5-H6⋯S3 | 2.76 | 0.0107 | 0.026 | 0.0003 | −7.5 |
| **NH$_2$S-3** | C1-H2⋯O7 | 2.19 | 0.0170 | 0.050 | 0 | −16.6 |
| | O8-H9⋯S3 | 2.23 | 0.0270 | 0.057 | 0 | −19.0 |

[a] The total electron energy density.
[b] Individual energy of each hydrogen bond.

HCOOH with XCHZ appears to be governed by the O8-H9⋯Z3 contacts, in which the O8-H9⋯O3 plays a larger role in complex stabilization.

### Interaction energy and role of energetic components in complexes

Interaction energies of the 36 complexes including only ZPE ($\Delta E$) and both ZPE + BSSE ($\Delta E^*$) corrections at the CCSD(T)/ aug-cc-pVDZ//MP2/aug-cc-pVDZ level are gathered in Table 3. Interaction energies range from −12.1 to −47.2 kJ mol$^{-1}$ without BSSE and −6.3 to −42.2 kJ mol$^{-1}$ with BSSE, indicating that obtained complexes are quite stable on the potential energy surface. A similar trend of change in strength of complexes emerges for values with and without BSSE correction. Consequently, only interaction energies corrected by both BSSE and ZPE are used in the following discussion.

We now consider the substituent effects of **X** and **Z** in XCHZ on stabilization energy of XCHZ⋯HCOOH complexes. Relationship of interaction energies with respect to various **X** and **Z** substitution in the complexes is plotted in Figure 4. Inspection of Table 3 and Figure 4 shows that for the same **X** and **Z**, a decreasing magnitude in complex stability is obtained in the ordering **XZ-3** > **XZ-1** > **XZ-2**. Thus, **XZ-3** is 10–15 kJ mol$^{-1}$ and 14–21 kJ mol$^{-1}$ lower in energy than **XZ-1** and **XZ-2**,
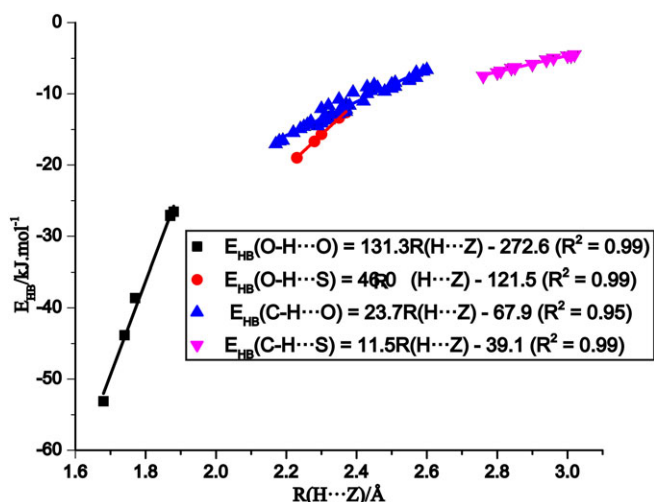


**Figure 2.** Linear dependence between individual hydrogen-bonded energies ($E_{HB}$, kJ mol$^{-1}$) and the intermolecular distances (R(H⋯Z), Å) for XCHZ⋯HCOOH (**X** = H, F, Cl, Br, CH$_3$, NH$_2$; **Z** = O, S). [Color figure can be viewed at wileyonlinelibrary.com]

respectively. Interestingly, with the alike **X** of **XO-n** for XCHO⋯HCOOH, intermolecular distances of H6/H9⋯O3 and H2⋯O7/O8 increase in the ordering: **XO-3** < **XO-2** < **XO-1** and **XO-3** < **XO-1** < **XO-2**, respectively. Such a trend is also similar to the case of **XS-n** for XCHS⋯HCOOH. It implies a larger role of the H2⋯O7/O8, relative to H6/H9⋯Z3 contacts, in stabilizing the **XZ-1** and **XZ-2** complexes, and the largest contribution to complex stability belongs to the O8-H9⋯Z3 contacts in **XZ-3**.

It is remarkable that for the alike **X** and **n**, **XO-n** is more stable than **XS-n**. This is consistent with the shorter corresponding distances of H2⋯O7/O8 and H6/H9⋯O3 in **XO-n** as compared to H2⋯O7/O8 and H6/H9⋯S3 in **XS-n**. The larger stability of **XO-n** versus **XS-n** arises from predominating contribution of attractive electrostatic interaction between O3 and H6/H9 atoms, overcoming that between S3 and H6/H9 atoms, and as a result, charge-transfer interaction does not play an important role in stabilizing the complexes. This observation results directly from a stronger polarizability of C-H bond and a larger gas phase basicity at S site in XCHS relative to XCHO, with the same **X**. Thus, the gas phase basicity is weaker at O site than at S site, and the polarity of C-H bond in XCHO is also weaker than that in XCHS (Table 1). Furthermore, the NBO analysis for isolated monomers listed in Table 1 shows that for the same **X**, the net charge is more negative for O site in XCHO than for S site in XCHS.

The most stable **XZ-3** complexes of XCHZ⋯HCOOH found in the present work have a strength lying between that of interactions of (HCHZ)$_2$ and (XCOOH)$_2$ dimers, with **Z** = O, S and **X** = H, CH$_3$. The interaction energy of the most stable complex of HCHO⋯HCHO amounts to −13.3 kJ mol$^{-1}$ at the CCSD(T)/CBS level,[50] and of HCHO⋯HCHO, HCHO⋯HCHS, and HCHS⋯HCHS is −12.3, −11.7, and −10.7 kJ mol$^{-1}$ by CCSD(T)-F12/heavy-aug-cc-pVTZ computations.[40] They are −21.03, and −22.4 kJ mol$^{-1}$ for HCHO⋯HCHO and CH$_3$CHO⋯CH$_3$CHO at MP2/aug-cc-pVTZ (with BSSE correction), respectively.[49] Very stable hydrogen-bonded interactions in HCOOH⋯HCOOH and CH$_3$COOH⋯CH$_3$COOH, with interaction energies of −56.9 and −60.7 kJ mol$^{-1}$ (taking BSSE into account) were obtained at MP2/6-311++G(d,p), respectively.[51] Besides, these complexes are more stable than the HNO⋯YCHZ (Y = H, F, Cl, Br, CH$_3$; Z = O, S) with interaction energies ranging from −9.5 to −13.6 kJ mol$^{-1}$ (both BSSE + ZPE corrections derived from MP2/aug-cc-pVTZ computations).[24]

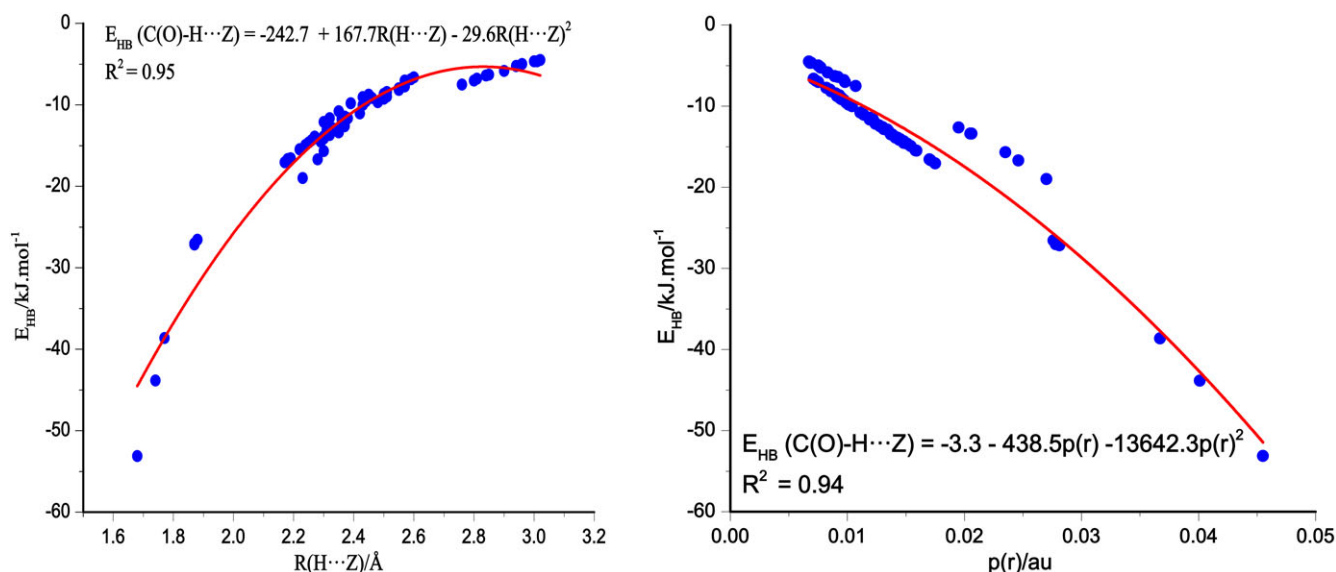We continue the discussion in more detail on the complex strength on the basis of influence of various substitutions.

**Figure 3.** The second-order correlation of individual hydrogen bond energies ($E_{HB}$) with respect to intermolecular distances (R(H⋯Z)) and electron density (ρ(r)) at BCPs for **XZ-n** (**X** = H, F, Cl, Br, $CH_3$, $NH_2$; **Z** = O, S; **n** = 1, 2, 3). [Color figure can be viewed at wileyonlinelibrary.com]

For all **XZ-1** complexes, interaction energies range from −9.7 to −15.6 kJ mol$^{-1}$ and with the same **Z**, they increase in the ordering **$NH_2$Z-1** < **BrZ-1** ≈ **ClZ-1** ≈ **FZ-1** < **$CH_3$Z-1** < **HZ-1**. As shown in Table 1, for both XCHO and XCHS, the gas phase basicity at O and S site is reduced in the ordering of $NH_2$ via $CH_3$ via H via Br via Cl and then to F; the polarity of C–H bond is decreased in going from Br to Cl to F to $NH_2$ to $CH_3$ and then to H. Consequently, the stabilization of **$NH_2$-1**, **BrZ-1**, **ClZ-1**, and **FZ-1** is mainly determined by the gas phase basicity at **Z** site, while the polarity of C-H bond plays a main role in stabilizing **$CH_3$Z-1** and **HZ-1**.

There is a small difference in tendency of stability for the case of **XZ-2** complexes, relative to **XZ-1** counterparts in which strength of **$CH_3$Z-2** lies between those of **BrZ-2** and **$NH_2$Z-2**. Hence, all **XZ-2** complexes are stabilized by a larger role of gas phase basicity at **Z** site, as compared to the polarity of C–H bond in XCHZ, except for the contribution of both factors in **HZ-2**. **XZ-3** is the most stable one among the three shapes of XCHZ⋯HCOOH complexes, with interaction energy ranging from −20.5 to −42.2 kJ mol$^{-1}$. For the same **Z**, the **XZ-3** complex strength tends to lessen in the ordering: **$NH_2$Z-3** > **$CH_3$Z-3** > **HZ-3** > **BrZ-3** **ClZ-3** **FZ-3**, indicating a larger role of gas phase basicity at **Z** site relative to polarity of C-H covalent bond in XCHZ.

In summary, substitution of one H atom in HCHZ by **X** (**X** = F, Cl, Br, $CH_3$, $NH_2$) results in an enhancement of stability of XCHZ⋯HCOOH relative to HCHZ⋯HCOOH for both shapes **XZ-1** and **XZ-2**. Nevertheless, for **XZ-3** shape, this replacement induces a significant increase in stability of the **$NH_2$Z-3** and **$CH_3$Z-3** complexes and causes a decrease of strength in halogenated complexes. The increase amounts to about 15 and 10 kJ mol$^{-1}$ for substituted formaldehydes and thioformaldehydes, respectively. Notably for the same **X**, the magnitude in strength of the complexes **XZ-n** (**X** = halogens) approximates for any shape.

To estimate the role of individual energy components contributing to the complex strength, SAPT2+ calculations in conjunction with the aug-cc-pVDZ basis set are carried out, and selected results are tabulated in Tables S2a and S2b, Supporting Information. The contribution percentages of different energy terms to the overall stabilization of the XCHO⋯HCOOH and XCHS⋯HCOOH complexes are displayed in Figures 5a and 5b. The contribution of attractive electrostatic component to the total stabilization energy of complex ranges from 41 to 55%, and is larger than that of dispersion and induction counterparts, which are around 13–31% and 17–33% respectively. Therefore, the former term overwhelming the two latter ones mainly

**Table 3.** Interaction energy (ΔE for only ZPE correction and ΔE$^*$ for both ZPE and BSSE correction, all in kJ mol$^{-1}$) of the complexes **XZ-n** at CCSD(T)/aug-cc-pVDZ//MP2/aug-cc-pVDZ.

| Complex | HO-1 | HO-2 | HO-3 | FO-1 | FO-2 | FO-3 | ClO-1 | ClO-2 | ClO-3 |
|---|---|---|---|---|---|---|---|---|---|
| ΔE | −15.5 | −12.1 | −33.9 | −19.1 | −13.2 | −31.4 | −19.2 | −13.6 | −31.2 |
| ΔE$^*$ | −11.2 | −7.9 | −27.0 | −13.9 | −8.5 | −24.0 | −14.0 | −8.6 | −24.1 |
| **Complex** | **BrO-1** | **BrO-2** | **BrO-3** | **$CH_3$O-1** | **$CH_3$O-2** | **$CH_3$O-3** | **$NH_2$O-1** | **$NH_2$O-2** | **$NH_2$O-3** |
| ΔE | −19.8 | −14.2 | −31.4 | −17.7 | −14.6 | −39.5 | −20.8 | −17.2 | −47.2 |
| ΔE$^*$ | −14.1 | −8.7 | −24.3 | −12.6 | −9.7 | −31.7 | −15.6 | −11.9 | −42.2 |
| **Complex** | **HS-1** | **HS-2** | **HS-3** | **FS-1** | **FS-2** | **FS-3** | **ClS-1** | **ClS-2** | **ClS-3** |
| ΔE | −15.4 | −12.1 | −29.9 | −18.2 | −13.2 | −28.9 | −18.9 | −14.2 | −30.5 |
| ΔE$^*$ | −9.7 | −6.3 | −21.8 | −11.9 | −7.0 | −20.5 | −12.0 | −7.3 | −21.1 |
| **Complex** | **BrS-1** | **BrS-2** | **BrS-3** | **$CH_3$S-1** | **$CH_3$S-2** | **$CH_3$S-3** | **$NH_2$S-1** | **$NH_2$S-2** | **$NH_2$S-3** |
| ΔE | −19.5 | −14.9 | −31.0 | −18.0 | −14.6 | −34.4 | −22.1 | −17.4 | −41.8 |
| ΔE$^*$ | −12.1 | −7.4 | −21.2 | −11.2 | −7.8 | −25.4 | −15.3 | −10.8 | −32.8 |
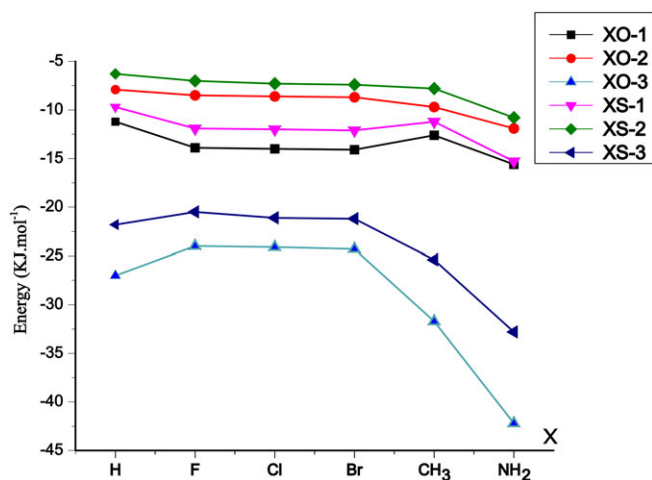
**Figure 4.** The relationship of the interaction energies and different X substitutions (**X** = H, F, Cl, Br, CH₃, NH₂) for XCHZ···HCOOH (**Z** = O, S). [Color figure can be viewed at wileyonlinelibrary.com]

contributes to the overall stabilization of all investigated complexes. In each complex of **XZ-1** and **XZ-2**, the dispersion component has a larger contribution, as compared to the induction component, to the overall complex energy. Nevertheless, a reverse trend is found in each complex of **XZ-3**, for which a larger role of the induction component is estimated.

A considerable value of 69–120 kJ mol$^{-1}$ due to exchange-repulsion term is about 1.5 times as large in absolute value as the attractive electrostatic term estimated in **XZ-3**, compared to the rest of the complexes. Furthermore, it tends to be enhanced in going from F to Cl to Br to H to CH₃ and to NH₂ substitution irrespective of **Z**. Subsequently, the exchange-repulsion energy is not fully quenched by the electrostatic interaction energy term.

As shown in Tables S2a and S2b, the contribution percentage of electrostatic term in the **XO-n** complexes is larger than that of **XS-n** ones, with the alike **X** and **n**, whereas the sum of percentage of dispersion and induction terms contributing to the stability of the former is smaller than that of the latter. This indicates a larger role of electrostatic energy in **XO-n** relative to **XS-n** in stabilizing the complexes. Interaction energies taken from the SAPT2+ approach range from −13 to −65 kJ mol$^{-1}$, and the complex stability is found to increase in the order of **XZ-2** via **XZ-1** and then to **XZ-3** for the same **X** and **Z**. Such a trend in complex stability is consistent with those derived from CCSD(T)/aug-cc-pVDZ computations.

### Changes of C-H and O-H bond lengths and their stretching frequencies

Changes of C1-H2, C5-H6, and O8-H9 bond lengths (Δ$r$, in Å) and their corresponding stretching frequency (Δ$\nu$, in cm$^{-1}$) are found in Table 4 (MP2/aug-cc-pVDZ values). Upon complexation, a C1-H2 contraction of 0.0001–0.0073 Å and an increase in its stretching frequency of 1–96 cm$^{-1}$ are observed in all the **XZ-n** complexes, except for **ClS-3** and **BrS-3** with a very slight C1-H2 elongation of 0.0007–0.0008 Å along with a stretching frequency decrease of 2–3 cm$^{-1}$. The C1-H2···O7/O8 hydrogen

bonds in **XZ-n** complexes thus belong to the BSHBs, except for the two complexes **ClS-3** and **BrS-3** being RSHBs. This exception should be designated to the largest polarity of the C-H bonds in the BrCHS and ClCHS monomers as compared to those in the rest of monomers (cf. Table 1). In general, for both alike **X** and **n**, a distance contraction and an increase in stretching frequencies of C1-H2 bonds in **XS-n** are smaller than those in **XO-n**. They are indeed 0.0001–0.0018 Å and 1–30 cm$^{-1}$ for the former and 0.0018–0.0073 Å and 26–96 cm$^{-1}$ for the latter. For the same proton acceptor, the weaker polarity of the C-H bond in the isolated monomer is, the larger contraction of C-H bond length and a blueshift of its stretching frequency upon complexation are, and vice versa.

Interestingly, following complexation, a very large C1-H2 contraction of 0.0058–0.0073 Å and its stretching frequency increase of 81–96 cm$^{-1}$ are observed for **HO-3**, **NH₂O-3**, and **CH₃O-3**. Such a considerable blueshift for C-H bond has not been ever reported, especially for a C$_{sp2}$-H bond. Our previous work indeed reported for C$_{sp2}$-H blueshifts in the C$_{sp2}$-H···O hydrogen bond by 12–27 cm$^{-1}$, 24–53 cm$^{-1}$ for the RCHO···CO₂ (MP2/aug-cc-pVT),[31] and RCHO···HNO (MP2/aug-cc-pVTZ)[24] with R = H, F, Cl, Br, CH₃. Very recently, the largest C$_{sp3}$-H blueshift of 35 and 50 cm$^{-1}$ was also evaluated for C$_{sp3}$-H···O in F₃CH···OHK and C$_{sp3}$-H···F in F₃CH···FK (with K = H, CH₃, at MP2/6-311++G (d,p)).[29] It is also surprising that a moderate increase of C1-H2 stretching frequency by 19–30 cm$^{-1}$ is estimated for **HS-3**, **NH₂S-3**, and **CH₃S-3**, even though there is only a slight difference in the polarity of the C-H bond in XCHO relative to XCHS (**X** = H, NH₂, CH₃). This result emphasizes a decisive role of the presence of the O8-H9···O3 as compared to the O8-H9···S3 hydrogen bond, besides polarity of C-H bond and gas phase basicity at **Z** site in isolated monomer, in effect on considerable changes of C1-H2 bond length as well as its stretching frequency following complexation. This phenomenon will be further considered in the subsequent section on NBO analysis.

For **XZ-1** and **XZ-2**, following complexation there are a length contraction and a stretching frequency increase of C5-H6 bond in the C5-H6···Z3 hydrogen bond of XCHZ···HCOOH complexes, except for **HS-2**, **CH₃S-2**, and **NH₂S-2** (cf. Table 4). Specifically, the C5-H6 bond length is shortened by 0.0001–0.0017 Å, accompanied by its stretching frequency enhancement of 1–26 cm$^{-1}$. The C5-H6 stretching frequency blueshifts are larger in magnitude for C5-H6···O3 than for C5-H6···S3, and this trend is also observed for each pair of the same **n** and **X** in **XZ-n** (**n** = 1, 2), which is consistent with the weaker gas phase basicity of O site in XCHO relative to S site in XCHZ (with the same **X**). Additionally, for the interaction of HCOOH with XCHO or XCHS, complex formation generally induces an increasing magnitude of C5-H6 blueshifts in the sequence of NH₂ via CH₃ via H via Br via Cl and to F substitution (cf. Table 4). These results again attest that for the same proton donor, the weaker the gas phase basicity of proton acceptor is, the larger the blueshift following complexation is, and vice versa.

All C5-H6 distances in the C5-H6···S3 hydrogen bonds are slightly shortened and blue-shifted upon complexation, which are only 0.0001–0.0010 Å and 1–13 cm$^{-1}$ for **XS-n** (**n** = 1–2), except for **HS-2**, **CH₃S-2**, and **NH₂S-2** with a slight elongation
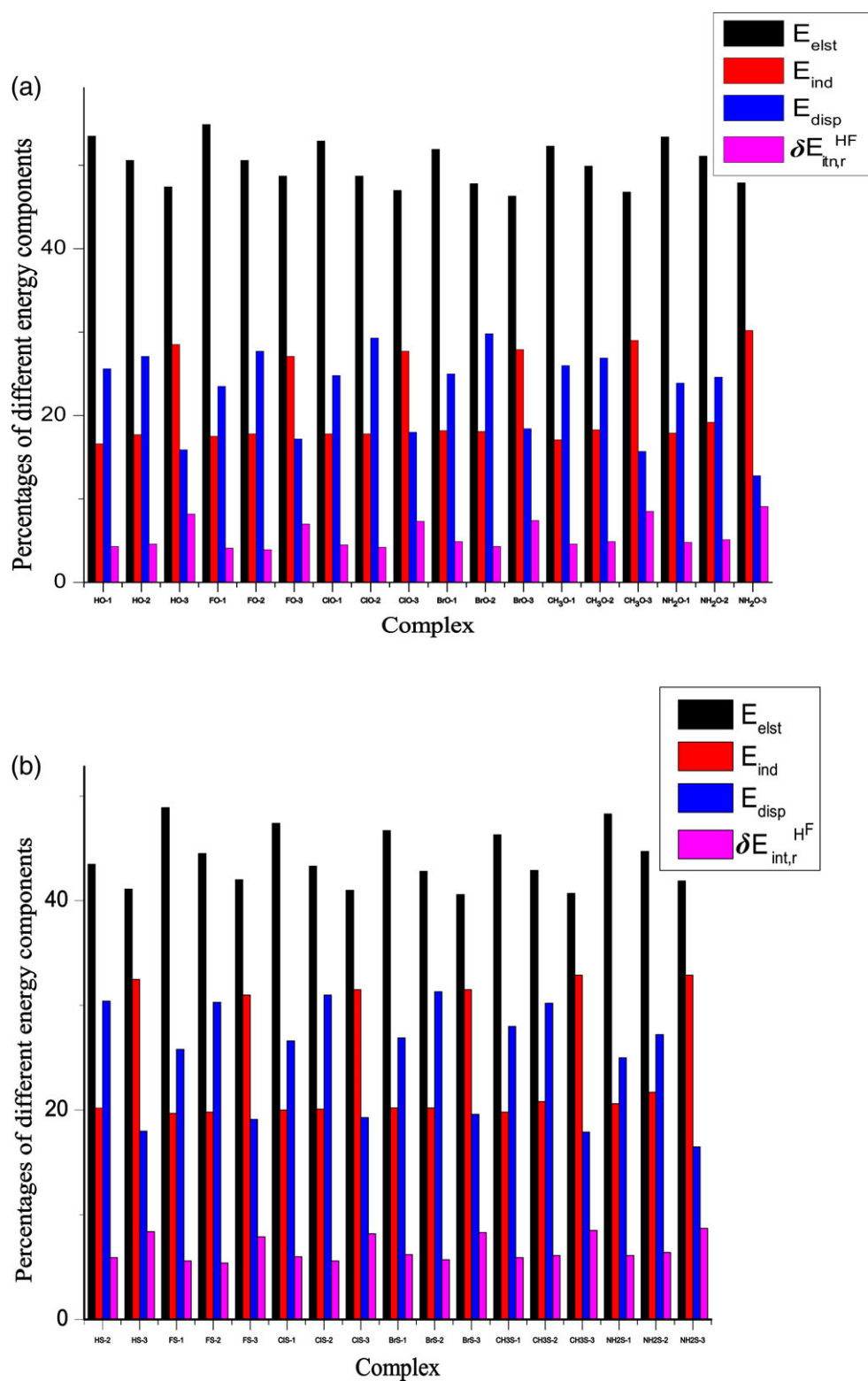
**Figure 5.** Diagram for contribution percentage of different energy components into total stabilization energy of the complexes for XCHO···HCOOH (Fig. 5a), XCHS···HCOOH (Fig. 5b) in the SAPT2+ approach, with **X** = H, F, Cl, Br, CH$_3$, NH$_2$. [Color figure can be viewed at wileyonlinelibrary.com]

of 0.0002–0.0005 Å and a negligible stretching frequency decrease of 1–5 cm$^{-1}$. Hence, the C5-H6···S3 hydrogen bonds in **HS-2**, **CH$_3$S-2** and **NH$_2$S-2** are RSHBs, and blue-shifted in all the remaining complexes. These blueshifts are comparable to those previously reported for the C-H···S hydrogen bond in CH$_2$F$_2$···H$_2$S and CH$_3$F···H$_2$S (MP2/aug-cc-pVDZ values).[38] A C-H shortening of 0.0003 Å and its stretching frequency

increase of 8 cm$^{-1}$ for CH$_4$···H$_2$S were observed, whereas a C-H elongation of 0.0006 Å concomitant accompanied by a decrease of its stretching frequency by 1.4 cm$^{-1}$ for C$_2$H$_4$···H$_2$S was reported.[35]

For **XZ-3**, all O8-H9···Z3 interactions belong to RSHBs, which result from a large elongation of O8-H9 distances of 0.0101–0.0271 Å and a significant decrease of its stretching

frequencies of 206–544 cm$^{-1}$. Such an increasing trend in magnitude of redshift is in good agreement with the enhancement of gas phase basicity at O or S site in the XCHO or XCHS monomers in going from F to Cl to Br to H to CH$_3$ and then to NH$_2$ substitution (cf. Tables 1 and 4). For the same proton donor, the stronger RSHB is obtained when the stronger gas phase basicity of proton acceptor, and vice versa. For each corresponding pair of **XO-3** and **XS-3**, the larger redshift associated with the O8-H9 bond is observed for the **XO-3** in the cases of H, CH$_3$ and NH$_2$ substitution (Table 4), while it is larger for the **XS-3** in the cases of F, Cl, and Br substitution. This observation will be clarified in a following section of NBO analysis.

Highly linear correlations of the changes of C1–H2, C5–H6, and O8-H9 stretching vibrational frequencies versus the changes of their corresponding bond lengths are presented in Figure S3, Supporting Information, and their correlation equations are expressed as follows:

$$\Delta\nu(\text{C1–H2}) \left(\text{cm}^{-1}\right) = -13124\,\Delta r\,(\text{C1–H2})\,(\text{Å}) + 2.39\,(R^2 = 0.96) \tag{1}$$

$$\Delta\nu(\text{C5–H6}) \left(\text{cm}^{-1}\right) = -14704\,\Delta r(\text{C5–H6})\,(\text{Å}) + 1.62\,(R^2 = 0.94) \tag{2}$$

$$\Delta\nu(\text{O8–H9}) \left(\text{cm}^{-1}\right) = -19848\,\Delta r(\text{O8–H9})\,(\text{Å}) - 14.03\,\left(R^2 = 0.99\right) \tag{3}$$

Negative slope and high correlation coefficients demonstrate that the $\Delta\nu$(C1-H2), $\Delta\nu$(C5-H6), and $\Delta\nu$(O8-H9) are in an excellently inverse correlation with the $\Delta r$(C1-H2), $\Delta r$(C5-H6), and $\Delta r$(O8-H9), respectively. The larger slope of eq. (3) as compared to those of eqs. (2) and (1) implies a greater sensitivity of the $\nu$(O8-H9) relative to the $\nu$(C5-H6) and $\nu$(C1-H2) stretching modes versus the variations of their corresponding bond lengths.

To consider quantitatively the effective role of both factors on the origin of the C-H···Z and O-H···Z hydrogen bonds, the ratio of DPE to PA (DPE/PA = **R$_c$**) which is proposed by our group as an indicator to predict the BSHB or RSHB[31] of C-H or O-H bond and Z atom in the relevant monomers for all the complexes is calculated and given in Table 4. The ratio **R$_c$** ranges from 1.7 to 2.5. In general, for C-H···Z hydrogen bonds, this indicator is slightly larger than, or equal to, 2.1 for BSHB and less than 2.1 for RSHB, except the C1-H2···O7 in **BrO-1** and **BrO-3** (**R$_c$** being 2.0), the C5-H6···O3 in **NH$_2$O-1** and **NH$_2$O-2** (**R$_c$** being 1.9), the C5-H6···S3 in **CH$_3$S-1** (**R$_c$** being 2.0), the C5-H6···S3 in **NH$_2$S-1** (**R$_c$** being 1.9) are blue-shifted, whereas the C5-H6···S3 in **HS-2** and C1-H2···O7 in **ClS-3** and **BrS-3** are red-shifted (**R$_c$** being 2.1). The **R$_c$** for the C–H···Z hydrogen bonds are larger than that for the O–H···Z hydrogen bonds, implying that the larger the **R$_c$** is, the larger expected BSHB is, and vice versa RSHB is predicted if the **R$_c$** is smaller. Our present results along with those in previous work[31] suggest that the **R$_C$** ratio can be used to probe the character and magnitude of hydrogen bond when the complex possesses one hydrogen bond. If the complex is stabilized by more than two hydrogen bonds, the role of remaining hydrogen bonds needs to be considered afterwards.

## NBO analysis

To attain a clearer view on the stability and origin of hydrogen bonds in the complexes, NBO analysis is performed at the MP2/aug-cc-pVDZ level and the selected results are gathered in Tables 5 and 6.

For the same **X** and **Z,** there is a very strong transfer of electron density going from n(Z3) to σ*(O8–H9) orbital in **XZ-3**, which is accounted for very large values of intermolecular hyperconjugative energies of n(Z3) → σ*(O8–H9) relative to n(Z3) → σ*(C5–H6) process in **XZ-1** and **XZ-2**. For each **XZ-n**, with the same **X** and **Z**, a dominating electron transfer from n(O7/O8) to σ*(C1–H2) orbital in **XZ-3** as compared to that in **XZ-1** and **XZ-2** is estimated. Thus, $E_{\text{inter}}$(n(O7/O8) → σ*(C1–H2)) is larger for **XZ-3** than for **XZ-1** and **XZ-2** (cf. Table 5). Therefore, both a loss of occupation of the σ*(C1–H2) orbital for **XO-n** and its larger decrement for **XO-3,** as compared to **XO-1** and **XO-2,** arise from a larger decrease of intramolecular transfer of electron density from the n(O3) to σ*(C1–H2)) orbital, overcoming an increase of its occupation taken from the n(O7/O8) to σ*(C1–H2) orbital, and a significant role of interaction of n(O3) → σ*(C1–H2) versus n(O7/O8) → σ*(C1–H2) for **XO-3** is assigned. On the other hand, as seen in Table 6, all values of Δσ*(C1–H2) for **XS-n** are slightly positive, implying an increase of electron density in the σ*(C1–H2) orbital following complexation. This indicates a predominating electron transfer from the n(O7/O8) to σ*(C1–H2) orbital over a decrease of σ*(C1–H2) occupation resulting from transfer of n(S3) to σ*(C1–H2). It is hence obvious that a stronger intermolecular interaction takes place from n(S3) to σ*(C5–H6) in **XS-1** and **XS-2** and n(S3) to σ*(O8–H9) in **XS-3** as compared to n(O3) to σ*(C5–H6) in **XO-1** and **XO-2** and n(O3) to σ*(O8–H9) in **XO-3**, and as a result, the interaction of n(O7/O8) → σ*(C1–H2) is stronger in **XS-n** than in **XO-n** for the same **X** and **n** (cf. Table 5). For this reason, an electron density transfer occurs from XCHZ to HCOOH in all complexes, except for **XZ-1** (**X** = F, Cl, Br).

Negative values of electron density transfer (EDT) are in the range of 0.0007–0.0548 electron, and positive values ranging from 0.0036 to 0.0053 electrons. This indicates that the interactions of n(Z3) → σ*(C5–H6) and n(Z3) → σ*(O8–H9) play a dominant role as compared to n(O7/O8) → σ*(C1–H2) in stabilizing the complexes, except for **XZ-1** (**X** = F, Cl, Br) with a larger role of the latter. The $E_{\text{inter}}$(n(O7/O8) → σ*(C1–H2)) is indeed larger than $E_{\text{inter}}$(n(Z3) → σ*(C5–H6)) in **XZ-1**. The importance of the interaction n(Z3) → σ*(O8–H9), relative to n(O7/O8) → σ*(C1–H2) and n(Z3) → σ*(C5–H6) can be proposed as very large negative EDT values are obtained for **XZ-3**.

For the same **X** and **Z**, along with changes in electron density of the σ*(C1–H2) orbital, an increase in s-character percentage of C1(H2) orbital in **XZ-n**, which is larger in magnitude for **XZ-3** than for **XZ-1** and **XZ-2**, is observed. Consequently, a C1–H2 bond contraction and a stretching frequency blueshift in the C1–H2···O7/O8 hydrogen bonds for **XO-n** are contributed by a decrease of population in σ*(C1–H2) orbital and an increase of

**Table 4.** Changes of bond length ($\Delta r$, in Å) and corresponding stretching frequency ($\Delta \nu$, in cm$^{-1}$) at MP2/aug-cc-pVDZ.

| Complex | HO-1 | HO-2 | HO-3 | FO-1 | FO-2 | FO-3 |
|---|---|---|---|---|---|---|
| $\Delta r$(C1-H2) | −0.0035 | −0.0024 | −0.0058 | −0.0021 | −0.0021 | −0.0024 |
| $\Delta r$(C5-H6)/$\Delta r$(O8-H9) | −0.0017 | −0.0011 | 0.0176 | −0.0016 | −0.0015 | 0.0101 |
| $\Delta \nu$(C1-H2) | 46 | 32 | 81 | 28 | 26 | 35 |
| $\Delta \nu$(C5-H6)/$\Delta \nu$(O8-H9) | 25 | 22 | −363 | 24 | 26 | −206 |
| $R_c$(C1-H2) | 2.3 | 2.5 | 2.3 | 2.1 | 2.4 | 2.1 |
| $R_c$(C5-H6)/$R_c$(O8-H9) | 2.3 | 2.3 | 2.1 | 2.4 | 2.4 | 2.2 |
| **Complex** | **ClO-1** | **ClO-2** | **ClO-3** | **BrO-1** | **BrO-2** | **BrO-3** |
| $\Delta r$(C1-H2) | −0.0022 | −0.0021 | −0.0021 | −0.0019 | −0.0019 | −0.0018 |
| $\Delta r$(C5-H6)/$\Delta r$(O8-H9) | −0.0015 | −0.0014 | 0.0104 | −0.0013 | −0.0013 | 0.0101 |
| $\Delta \nu$(C1-H2) | 33 | 29 | 37 | 30 | 26 | 33 |
| $\Delta \nu$(C5-H6)/$\Delta \nu$(O8-H9) | 22 | 24 | −215 | 20 | 22 | −210 |
| $R_c$(C1-H2) | 2.1 | 2.3 | 2.1 | 2.0 | 2.2 | 2.0 |
| $R_c$(C5-H6)/$R_c$(O8-H9) | 2.3 | 2.3 | 2.1 | 2.3 | 2.3 | 2.1 |
| **Complex** | **CH$_3$O-1** | **CH$_3$O-2** | **CH$_3$O-3** | **NH$_2$O-1** | **NH$_2$O-2** | **NH$_2$O-3** |
| $\Delta r$(C1-H2) | −0.0040 | −0.0029 | −0.0073 | −0.0031 | −0.0024 | −0.0064 |
| $\Delta r$(C5-H6)/$\Delta r$(O8-H9) | −0.0013 | −0.0008 | 0.0210 | −0.0010 | −0.0007 | 0.0271 |
| $\Delta \nu$(C1-H2) | 54 | 39 | 96 | 44 | 34 | 85 |
| $\Delta \nu$(C5-H6)/$\Delta \nu$(O8-H9) | 20 | 18 | −432 | 18 | 17 | −544 |
| $R_c$(C1-H2) | 2.2 | 2.5 | 2.2 | 2.2 | 2.5 | 2.2 |
| $R_c$(C5-H6)/$R_c$(O8-H9) | 2.1 | 2.1 | 1.9 | 1.9 | 1.9 | 1.8 |
| **Complex** | **HS-1** | **HS-2** | **HS-3** | **FS-1** | **FS-2** | **FS-3** |
| $\Delta r$(C1-H2) | −0.0005 | −0.0006 | −0.0008 | −0.0001 | −0.0005 | −0.0002 |
| $\Delta r$(C5-H6)/$\Delta r$(O8-H9) | −0.0006 | 0.0002 | 0.0149 | −0.0010 | −0.0003 | 0.0106 |
| $\Delta \nu$(C1-H2) | 13 | 13 | 19 | 4 | 11 | 5 |
| $\Delta \nu$(C5-H6)/$\Delta \nu$(O8-H9) | 7 | −1 | −316 | 13 | 7 | −226 |
| $R_c$(C1-H2) | 2.2 | 2.4 | 2.2 | 2.1 | 2.4 | 2.1 |
| $R_c$(C5-H6)/$R_c$(O8-H9) | 2.1 | 2.1 | 1.9 | 2.2 | 2.2 | 2.0 |
| **Complex** | **ClS-1** | **ClS-2** | **ClS-3** | **BrS-1** | **BrS-2** | **BrS-3** |
| $\Delta r$(C1-H2) | −0.0002 | −0.0007 | 0.0007 | −0.0003 | −0.0007 | 0.0008 |
| $\Delta r$(C5-H6)/$\Delta r$(O8-H9) | −0.0008 | 0 | 0.0118 | −0.0007 | −0.0001 | 0.0118 |
| $\Delta \nu$(C1-H2) | 2 | 13 | −2 | 1 | 14 | −4 |
| $\Delta \nu$(C5-H6)/$\Delta \nu$(O8-H9) | 11 | 3 | −252 | 9 | 1 | −252 |
| $R_c$(C1-H2) | 2.1 | 2.3 | 2.1 | 2.1 | 2.3 | 2.1 |
| $R_c$(C5-H6)/$R_c$(O8-H9) | 2.1 | 2.1 | 1.9 | 2.1 | 2.1 | 1.9 |
| **Complex** | **CH$_3$S-1** | **CH$_3$S-2** | **CH$_3$S-3** | **NH$_2$S-1** | **NH$_2$S-2** | **NH$_2$S-3** |
| $\Delta r$(C1-H2) | −0.0013 | −0.0012 | −0.0018 | −0.0008 | −0.0009 | −0.0012 |
| $\Delta r$(C5-H6)/$\Delta r$(O8-H9) | −0.0003 | 0.0004 | 0.0167 | −0.0002 | 0.0005 | 0.0207 |
| $\Delta \nu$(C1-H2) | 22 | 21 | 30 | 15 | 17 | 21 |
| $\Delta \nu$(C5-H6)/$\Delta \nu$(O8-H9) | 4 | −4 | −352 | 3 | −5 | −430 |
| $R_c$(C1-H2) | 2.2 | 2.4 | 2.2 | 2.2 | 2.4 | 2.2 |
| $R_c$(C5-H6)/$R_c$(O8-H9) | 2.0 | 2.0 | 1.8 | 1.9 | 1.9 | 1.7 |

DPE/PA = $R_c$, the values of DPE and PA taken from Table 1; all values for the C–H and O–H bond involved in hydrogen bond.

$s$-character percentage of C1(H2) orbital. However, a C1–H2 bond contraction concomitant with its stretching frequency blueshift in C1–H2···O7/O8 hydrogen bonds for **XS-n** is governed by an increase of $s$-character percentage of C1(H2) atom overcoming that of $\sigma$*(C1–H2) electron density, and a slightly redshift of C1-H2 stretching frequency in **ClS-3** and **BrS-3** is determined by an increase in occupation of the $\sigma$*(C1-H2) orbital.

Following complexation, an increase of $s$-character percentage of C5(H6) orbital and a larger enhancement occur in **XZ-2** relative **XZ-1**, with the alike **X** and **Z**. A decrease of $\sigma$*(C5–H6) occupation is larger in **XO-1** relative to **XO-2**. However, a contrasting trend is observed when O atom is substituted by S atom, with a larger increase of $\sigma$*(C5–H6) occupation in **XS-2** as compared to **XS-1**. As shown in Table 5, $E_{inter}$(n(Z3) → $\sigma$*(C5–H6)) is larger for **XZ-2** than for **XZ-1**, with the same **X** and **Z**, and with the same **X** and **n**, $E_{inter}$(n(S3) → $\sigma$*(C5–H6)) is larger than $E_{inter}$(n(O3) → $\sigma$*(C5–H6)). This outcome results in a stronger gas

phase basicity of S site in XCHS versus O site in XCHO, with the same **X**. Consequently, for **XO-1** and **XO-2**, the larger magnitude of C5–H6 blueshift in the C5–H6···O3 hydrogen bond is contributed by two factors, namely, a decrease in electron density in $\sigma$*(C5–H6) orbital and an increase of $s$-character percentage of C5(H6)) hybridized orbital. However, a $s$-character increase of C5(H6) atom involving hydrogen bond overwhelming an increase of $\sigma$*(C5–H6) occupation results in a slight blueshift of C5–H6 stretching frequency in **XS-1** and **XS-2**. The C5–H6···S3 RSHB with a very weak shift of C5–H6 stretching frequency in **HS-2**, **CH$_3$S-2**, and **NH$_2$S-2** is caused by a large gain in $\sigma$*(C5–H6) electron density dominating an $s$-character enhancement of C5(H6) orbital.

Due to complexation, a considerable gain in occupation of $\sigma$*(O8–H9) orbital and an increase in $s$-character percentage of O8(H9) atom take place in **XZ-3**. In particular, the corresponding enhancement of both properties is 0.0255–0.0540 electron and 3–5% for **XO-3**, and 0.0384–0.0630 electron and 3–4%

**Wiley Online Library**

*J. Comput. Chem.* **2019**, *40*, 1387–1400     **1397**

**Table 5.** Hyperconjugative interaction energies (in kJ mol$^{-1}$) for the obtained complexes at MP2/aug-cc-pVDZ, with **X** = F, Cl, Br.

| Complex | HO-1 | HO-2 | HO-3 | FO-1 | FO-2 | FO-3 | ClO-1 | ClO-2 | ClO-3 |
|---|---|---|---|---|---|---|---|---|---|
| EDT | −0.0048 | −0.0084 | −0.0403 | 0.0036 | −0.0005 | −0.0196 | 0.0040 | −0.0007 | −0.0196 |
| $E_{intra}$(n(O3)) → σ*(C1-H2)) | 112.2 | 100.2 | 82.8 | 100.2 | 104.0 | 91.5 | 102.9 | 107.3 | 94.2 |
| $E_{intra}$(n(X) → σ*(C1-H2)) | – | – | – | 24.6 | 25.4 | 26.4 | 16.2 | 17.1 | 18.8 |
| $E_{inter}$(n(O7/O8) → σ*(C1-H2)) | 7.2 | 3.9 | 15.0 | 11.6 | 7.7 | 13.0 | 11.5 | 6.8 | 13.1 |
| $E_{inter}$(n(O3) → σ*(C5-H6/O8-H9)) | 11.3 | 14.5 | 103.7 | 7.7 | 8.8 | 66.5 | 5.6 | 6.9 | 64.8 |
| **Complex** | **BrO-1** | **BrO-2** | **BrO-3** | **CH$_3$O-1** | **CH$_3$O-2** | **CH$_3$O-3** | **NH$_2$O-1** | **NH$_2$O-2** | **NH$_2$O-3** |
| EDT | 0.0046 | −0.0007 | −0.0190 | −0.0048 | −0.0084 | −0.0436 | −0.0052 | −0.0090 | −0.0501 |
| $E_{intra}$(n(O3)) → σ*(C1-H2)) | 100.6 | 105.6 | 93.1 | 26.55 | 111.1 | 91.5 | 113.7 | 118.8 | 92.2 |
| $E_{intra}$(n(X) → σ*(C1-H2)) | 11.3 | 12.0 | 13.5 | – | – | – | – | – | – |
| $E_{inter}$(n(O7/O8) → σ*(C1-H2)) | 12.1 | 6.8 | 13.0 | 7.8 | 4.6 | 12.3 | 8.8 | 5.2 | 13.9 |
| $E_{inter}$(n(O3) → σ*(C5-H6/O8-H9)) | 5.3 | 7.7 | 62.4 | 13.5 | 17.0 | 118.7 | 16.9 | 20.6 | 148.0 |
| **Complex** | **HS-1** | **HS-2** | **HS-3** | **FS-1** | **FS-2** | **FS-3** | **ClS-1** | **ClS-2** | **ClS-3** |
| EDT | −0.0052 | −0.0112 | −0.0493 | 0.0036 | −0.0028 | −0.0294 | 0.0046 | −0.0028 | −0.0313 |
| $E_{intra}$(n(S3)) → σ*(C1-H2)) | 58.6 | 61.6 | 51.9 | 62.0 | 65.2 | 57.6 | 63.6 | 67.2 | 58.7 |
| $E_{intra}$(n(X) → σ*(C1-H2)) | – | – | – | 29.5 | 30.5 | 30.6 | 23.3 | 24.4 | 24.9 |
| $E_{inter}$(n(O7/O8) → σ*(C1-H2)) | 12.3 | 6.7 | 16.3 | 17.9 | 11.0 | 20.2 | 20.0 | 11.9 | 22.8 |
| $E_{inter}$(n(S3) → σ*(C5-H6/O8-H9)) | 16.2 | 21.1 | 100.2 | 10.1 | 14.5 | 73.0 | 11.1 | 15.2 | 78.0 |
| **Complex** | **BrS-1** | **BrS-2** | **BrS-3** | **CH$_3$S-1** | **CH$_3$S-2** | **CH$_3$S-3** | **NH$_2$S-1** | **NH$_2$S-2** | **NH$_2$S-3** |
| EDT | 0.0053 | −0.0026 | −0.0310 | −0.0038 | −0.0099 | −0.0497 | −0.0040 | −0.0110 | −0.0548 |
| $E_{intra}$(n(S3)) → σ*(C1-H2)) | 62.8 | 67.2 | 59.2 | 69.3 | 67.6 | 56.0 | 63.4 | 68.8 | 56.5 |
| $E_{intra}$(n(X) → σ*(C1-H2)) | 13.6 | 18.5 | 19.3 | – | – | – | – | – | – |
| $E_{inter}$(n(O7/O8) → σ*(C1-H2)) | 20.8 | 12.1 | 23.0 | 13.1 | 7.6 | 18.6 | 15.9 | 9.1 | 23.2 |
| $E_{inter}$(n(S3) → σ*(C5-H6/O8-H9)) | 10.9 | 14.9 | 18.31 | 76.6 | 23.1 | 108.9 | 21.5 | 26.7 | 126.7 |

$E_{inter}$ and $E_{intra}$ denoted for corresponding intermolecular and intramolecular hyperconjugative interaction energies.

for **XS-3**. It is also notable that for both **XO-3** and **XS-3**, the increase in electron density of σ*(O8-H9) orbital is larger for the H, CH$_3$, NH$_2$ than the halogen F, Cl, Br substitution (cf. Table 6), and as shown above, the larger redshift is obtained for the former than for the latter. It implies that very large elongation of O8-H9 distance and very large decrease of its stretching frequency depend on the relevant increase of σ*(O8-H9) orbital occupation upon complexation.

For the same **X** of **XO-3** and **XS-3**, the occupation of σ*(O8-H9) orbitals is enhanced in the ordering of F to Cl to Br to H to CH$_3$ and then to NH$_2$, which is consistent with the increasing tendency of gas phase basicity at O site in XCHO or S site in XCHS, and its increasing magnitude is larger for **XS-3** than for **XO**-3 (arising from gas phase basicity of S site larger O site). Therefore, the stronger redshift of O8-H9 stretching frequency for **XO-3** as compared to **XS-3** (**X** = H, CH$_3$, NH$_2$) can be attributed to a larger role of *s*-character of O8(H9) atom in the latter with respect to the former. Contrastingly, a larger contribution of change of σ*(O8-H9) occupation can be suggested for the larger elongation and

**Table 6.** Changes of electron density (Δσ*, in electron) and s-character percentage (Δ%s, in %) of atoms involving hydrogen bond from NBO analysis at MP2/aug-cc-pVDZ.

| Complex | HO-1 | HO-2 | HO-3 | FO-1 | FO-2 | FO-3 | ClO-1 | ClO-2 | ClO-3 |
|---|---|---|---|---|---|---|---|---|---|
| Δσ*(C1-H2) | −0.0045 | −0.0031 | −0.0084 | −0.0020 | −0.0006 | −0.0043 | −0.0026 | −0.0010 | −0.0041 |
| Δσ*(C5-H6) | −0.0023 | −0.0009 | – | −0.0029 | −0.0020 | – | −0.0027 | −0.0017 | – |
| Δσ*(O8-H9) | – | – | 0.0412 | – | – | 0.0255 | – | – | 0.0268 |
| Δ%s(C1) | 0.86 | 0.53 | 1.32 | 0.91 | 0.52 | 1.05 | 1.04 | 0.53 | 0.84 |
| Δ%s(C5/O8) | 0.89 | 1.21 | 4.02 | 0.58 | 0.96 | 3.29 | 0.55 | 0.91 | 3.22 |
| **Complex** | **BrO-1** | **BrO-2** | **BrO-3** | **CH$_3$O-1** | **CH$_3$O-2** | **CH$_3$O-3** | **NH$_2$O-1** | **NH$_2$O-2** | **NH$_2$O-3** |
| Δσ*(C1-H2) | −0.0026 | −0.0010 | −0.0038 | −0.0048 | −0.0028 | −0.0095 | −0.0045 | −0.0026 | −0.0101 |
| Δσ*(C5-H6) | −0.0026 | −0.0015 | – | −0.0020 | −0.0007 | – | −0.0023 | −0.0012 | – |
| Δσ*(O8-H9) | – | – | 0.0264 | – | – | 0.0469 | – | – | 0.0540 |
| Δ%s(C1) | 1.14 | 0.57 | 0.78 | 0.85 | 0.50 | 1.41 | 0.85 | 0.52 | 1.51 |
| Δ%s(C5/O8) | 0.52 | 0.88 | 3.13 | 1.09 | 1.37 | 4.38 | 1.29 | 1.63 | 4.89 |
| **Complex** | **HS-1** | **HS-2** | **HS-3** | **FS-1** | **FS-2** | **FS-3** | **ClS-1** | **ClS-2** | **ClS-3** |
| Δσ*(C1-H2) | 0.0003 | 0.0003 | 0.0001 | 0.0005 | 0.0012 | 0.0004 | 0.0009 | 0.0011 | 0.0013 |
| Δσ*(C5-H6) | 0.0022 | 0.0048 | – | 0.0003 | 0.0028 | – | 0.0006 | 0.0033 | – |
| Δσ*(O8-H9) | – | – | 0.0525 | – | – | 0.0384 | – | – | 0.0424 |
| Δ%s(C1) | 1.13 | 0.74 | 1.54 | 1.31 | 0.86 | 1.64 | 1.46 | 0.94 | 1.67 |
| Δ%s(C5/O8) | 0.74 | 0.99 | 3.78 | 0.50 | 0.80 | 3.17 | 0.54 | 0.82 | 3.32 |
| **Complex** | **BrS-1** | **BrS-2** | **BrS-3** | **CH$_3$S-1** | **CH$_3$S-2** | **CH$_3$S-3** | **NH$_2$S-1** | **NH$_2$S-2** | **NH$_2$S-3** |
| Δσ*(C1-H2) | 0.0013 | 0.0012 | 0.0015 | 0.0003 | 0.0008 | 0 | 0.0005 | 0.0009 | 0.0002 |
| Δσ*(C5-H6) | 0.0007 | 0.0034 | – | 0.0025 | 0.0048 | – | 0.0018 | 0.0044 | – |
| Δσ*(O8-H9) | – | – | 0.0424 | – | – | 0.0562 | – | 0.0008 | 0.0630 |
| Δ%s(C1) | 1.52 | 0.98 | 1.64 | 1.13 | 0.72 | 1.59 | 1.19 | 0.77 | 1.77 |
| Δ%s(C5/O8) | 0.53 | 0.53 | 3.43 | 0.87 | 1.11 | 4.05 | 1.09 | 1.40 | 4.53 |

redshift of O8–H9 bond in **XS-3** as compared to **XO-3** (**X** = F, Cl, Br).

## Conclusions

Interactions of formic acid (HCOOH) with substituted formaldehydes (XCHO) and thioformaldehydes (XCHS) induce 36 stable complexes with binding energies of 6.3–42.2 kJ mol$^{-1}$ as computed at the CCSD(T)/aug-cc-pVDZ//MP2/aug-cc-pVDZ level with ZPE and BSSE corrections. The overall stabilization of a complex is contributed by hydrogen bonds, and the largest role belongs to the O-H···Z (**Z** = O, S) hydrogen bond.

For the same **X**, substitution makes XCHS···HCOOH less stable than XCHO···HCOOH complex. For the same **X** and **Z**, the complex stability increases in the ordering of **XZ-2** to **XZ-1** and then to **XZ-3**, and the last one is 10–15 kJ mol$^{-1}$, 14–21 kJ mol$^{-1}$ lower in energy than the first and second one, respectively. The obtained results show that replacement of **X** by CH$_3$ and NH$_2$ induces an increase in stability of XCHO···HCOOH and XCHS···HCOOH as compared to the parent complexes HCHO···HCOOH and HCHS···HCOOH, respectively, while it causes a slight decrease of the complex strength when **X** is replaced by F, Cl, and Br.

The SAPT2+ results indicate that the attractive electrostatic term of 41–55% is dominant over the dispersion and induction counterparts of 13–33% and thus plays a main role in stabilizing the complexes, and the electrostatic term is larger for **XO-n** than for **XS-n**. Exchange-repulsion energy is not fully quenched by attractive electrostatic energy in complex stabilization.

A considerable bond contraction and frequency blueshift of C$_{sp2}$–H bond in the C$_{sp2}$–H···O hydrogen bond are observed following complexation, up to 0.0073 Å and 96 cm$^{-1}$, and a large elongation of O–H bond, and significant redshift of its stretching frequency, up to 0.0271 Å and 544 cm$^{-1}$ have been discovered. Such C$_{sp2}$–H blueshift and O–H redshift are due to a dependence on polarity of proton donor and gas phase basicity of proton acceptor involving hydrogen bond, and the rearrangement of electron density when the complex is formed. Our previous and present works evidently support the point of view that for the same proton donor, the weaker the gas phase basicity of proton acceptor, the larger the blueshift following complexation, and vice versa.

NBO analysis shows that the significant elongation of O8–H9 distance and the very large decrease of its stretching frequency arise from a considerable increase of the σ*(O8–H9) orbital. Some interesting correlations are also obtained that points out again a linear correlation between bond distance changes and frequency shifts.

## Acknowledgments

[1] G. Chalasinski, M. M. Szczesniak, *Chem. Rev.* **2001**, *100*, 4227.
[2] G. R. Desiraju, T. Steiner, The Weak Hydrogen Bond in Structural Chemistry and Biology, Oxford University Press Inc., New York, **1999**.
[3] S. J. Grabowski, In Series Challenges and Advances in Computational Chemistry and Physics; J. Leszczynski, Ed.; Springer: New York, **2006**.
[4] Y. Mandel-Gutfreund, H. Margalit, R. L. Jernigan, V. B. Zhurkin, *J. Mol. Biol.* **1998**, *277*, 1129.
[5] D. J. Olivier, F. Marc, C. Enric, *Chem. A Eur. J.* **2001**, *7*, 2635.
[6] J. J. J. Dom, B. Michielsen, B. U. W. Maes, W. A. Herrebout, B. J. van der Veken, *Chem. Phys. Lett.* **2009**, *469*, 85.
[7] J. M. Hermida-Ramon, A. M. Grana, *J. Comput. Chem.* **2007**, *28*, 540.
[8] C. D. Keefe, M. Isenor, *J. Phys. Chem. A* **2008**, *112*, 3127.
[9] R. Reddi, K. K. Singarapu, D. Pal, A. Addlagatta, *Mol. Biosyst.* **2016**, *12*, 2408.
[10] J. Joseph, E. D. Jemmis, *J. Am. Chem. Soc.* **2007**, *129*, 4620.
[11] I. V. Alabugin, M. Manoharan, S. Peabody, F. Weinhold, *J. Am. Chem. Soc.* **2003**, *125*, 5973.
[12] P. Hobza, Z. Havlas, *Chem. Rev.* **2000**, *100*, 4253.
[13] M. Budesinsky, P. Fiedler, Z. Arnold, *Synthesis* **1989**, *11*, 858.
[14] R. Taylor, O. Kennard, *J. Am. Chem. Soc.* **1982**, *104*, 5063.
[15] G. R. Desiraju, *Acc. Chem. Res.* **1991**, *24*, 290.
[16] A. Masunov, J. J. Dannenberg, R. H. Contreras, *J. Phys. Chem. A* **2001**, *105*, 4737.
[17] B. G. Oliveira, R. C. M. U. de Araújo, M. N. Ramos, *J. Mol. Struct. Theochem.* **2009**, *908*, 79.
[18] B. Reimann, K. Buchfold, S. Vaupel, B. Brutschy, Z. Havlas, V. Spirko, P. Hobza, *J. Phys. Chem. A* **2001**, *105*, 5560.
[19] P. Hobza, Z. Havlas, *Chem. Phys. Lett.* **1999**, *303*, 447.
[20] R. Gopi, N. Ramanathan, K. Sundararajan, *Spectrochim. Acta A* **2017**, *18*, 137.
[21] P. Hobza, J. Sponer, E. Cubero, M. Orozco, F. J. Luque, *J. Phys. Chem. B* **2000**, *104*, 6286.
[22] O. O. Brovarets, Y. P. Yurenko, D. M. Hovorun, *J. Biomol. Struct. Dyn.* **2014**, *32*, 993.
[23] Y. P. Yurenko, R. O. Zhurakivsky, S. P. Samijlenko, D. M. Hovorun, *J. Biomol. Struct. Dyn.* **2011**, *29*, 51.
[24] N. T. Trung, T. T. Hue, M. T. Nguyen, *J. Phys. Chem. A* **2009**, *113*, 3245.
[25] H. Q. Dai, N. N. Tri, N. T. T. Trang, N. T. Trung, *RSC Adv.* **2014**, *4*, 13901.
[26] O. Donoso-Tauda, P. Jaque, J. C. Santos, *Phys. Chem. Chem. Phys.* **2011**, *13*, 1552.
[27] X. Li, L. Liu, H. B. Schlegel, *J. Am. Chem. Soc.* **2002**, *124*, 9639.
[28] Y. Mo, C. Wang, L. Guan, B. Braïda, P. C. Hiberty, W. Wu, *Chem. A Eur. J.* **2014**, *20*, 8444.
[29] X. Chang, Y. Zhang, X. Weng, P. Su, W. Wu, Y. Mo, *J. Phys. Chem. A* **2016**, *120*, 2749.
[30] N. T. Trung, T. T. Hue, N. M. Tho, *Phys. Chem. Chem. Phys.* **2009**, *11*, 926.
[31] N. T. Trung, N. P. Hung, T. T. Hue, N. M. Tho, *Phys. Chem. Chem. Phys.* **2011**, *13*, 14033.
[32] N. T. H. Man, P. L. Nhan, V. Vien, D. T. Quang, N. T. Trung, *Int. J. Quantum. Chem.* **2017**, *117*, e25338.
[33] N. T. Trung, N. T. T. Trang, V. T. Ngan, D. T. Quang, N. M. Tho, *RSC Adv.* **2016**, *6*, 31401.
[34] N. N. Tri, N. T. H. Man, N. L. Tuan, N. T. T. Trang, D. T. Quang, N. T. Trung, *Theor. Chem. Acc.* **2017**, *10*, 136.
[35] G. Trudeau, J. M. Dumas, P. Dupuis, M. Guerin, C. Sandorfy, *Top. Curr. Chem.* **1980**, *93*, 91.
[36] M. Domagała, S. J. Grabowski, *J. Phys. Chem. A* **2005**, *109*, 5683.
[37] E. J. Cocinero, R. Sa´nchez, S. Blanco, A. Lesarri, J. C. Lo´pez, J. L. Alonso, *Chem. Phys. Lett.* **2005**, *402*, 4.
[38] M. Domagała, S. J. Grabowski, *Chem. Phys.* **2010**, *367*, 1.
[39] M. C. Rovira, J. J. Novoa, *Chem. Phys. Lett.* **1997**, *279*, 140.
[40] E. V. Dornshuld, C. M. Holy, G. S. Tschumper, *J. Phys. Chem. A* **2014**, *118*, 3376.

**Wiley Online Library**

*J. Comput. Chem.* **2019**, *40*, 1387–1400    **1399**

Journal of **COMPUTATIONAL CHEMISTRY**

[41] NIST Webpage: http://webbook.nist.gov/chemistry/

[42] S. F. Boys, F. Bernadi, *Mol. Phys.* **1970**, *19*, 553.

[43] M. J. Frisch, G. W. Trucks, H. B. Schlegel, G. E. Scuseria, M. A. Robb, J. R. Cheeseman, G. Scalmani, V. Barone, B. Mennucci, G. A. Petersson, H. Nakatsuji, M. Caricato, X. Li, H. P. Hratchian, A. F. Izmaylov, J. Bloino, G. Zheng, J. L. Sonnenberg, M. Hada, M. Ehara, K. Toyota, R. Fukuda, J. Hasegawa, M. Ishida, T. Nakajima, Y. Honda, O. Kitao, H. Nakai, T. Vreven, J. A. Montgomery, Jr., J. E. Peralta, F. Ogliaro, M. Bearpark, J. J. Heyd, E. Brothers, K. N. Kudin, V. N. Staroverov, R. Kobayashi, J. Normand, K. Raghavachari, A. Rendell, J. C. Burant, S. S. Iyengar, J. Tomasi, M. Cossi, N. Rega, J. M. Millam, M. Klene, J. E. Knox, J. B. Cross, V. Bakken, C. Adamo, J. Jaramillo, R. Gomperts, R. E. Stratmann, O. Yazyev, A. J. Austin, R. Cammi, C. Pomelli, J. W. Ochterski, R. L. Martin, K. Morokuma, V. G. Zakrzewski, G. A. Voth, P. Salvador, J. J. Dannenberg, S. Dapprich, A. D. Daniels, O. Farkas, J. B. Foresman, J. V. Ortiz, J. Cioslowski, and D. J. Fox, Gaussian 09 (version A.01), Inc., Wallingford CT, **2009**.

[44] J. M. Turney, A. C. Simmonett, R. M. Parrish, E. G. Hohenstein, F. A. Evangelista, J. T. Fermann, B. J. Mintz, L. A. Burns, J. J. Wilke, M. L. Abrams, N. J. Russ, M. L. Leininger, C. L. Janssen, E. T. Seidl, Q. D. Allen, H. F. Schaefer, R. A. King, E. F. Valeev, C. D. Sherrill, T. D. Crawford, *WIREs Comput. Mol. Sci.* **2012**, *2*, 556.

[45] W. J. F. Bader, *Chem. Rev.* **1991**, *91*, 893.

[46] E. Espinosa, E. Molins, C. Lecomte, *Chem. Phys. Lett.* **1998**, *285*, 170.

[47] I. Mata, I. Alkorta, E. Espinosa, E. Molins, *Chem. Phys. Lett.* **2011**, *507*, 185.

[48] E. D. Glendening, J. K. Badenhoop, A. E. Read, J. E. Carpenter, J. A. Bohmann, F. Weinhold, GenNBO 5.G, Theoretical Chemistry Institute; University of Wisconsin: Madison, WI, **1996**.

[49] I. V. Alabugin, S. Bresch, M. Manoharan, *J. Phys. Chem. A* **2014**, *118*, 3663.

[50] T. S. Thakul, M. T. Kirchner, D. Blaser, R. Boese, G. R. Desiraju, *Phys. Chem. Chem. Phys.* **2011**, *13*, 14076.

[51] G. A. Dolgonos, *Chem. Phys. Lett.* **2013**, *585*, 37.

[52] R. W. Gora, S. J. Grabowski, J. Leszczynski, *J. Phys. Chem. A* **2005**, *109*, 6397.

[53] U. Koch, P. L. A. Popelier, *J. Phys. Chem. A* **1995**, *99*, 9747.

[54] W. D. Arnold, E. Oldfield, *J. Am. Chem. Soc.* **2000**, *122*, 12835.

[55] I. Rozas, I. Alkorta, J. Elguero, *J. Am. Chem. Soc.* **2000**, *122*, 11154.